International Journal of Science and Research (IJSR)
ISSN (Online): 2319-7064
Index Copernicus Value (2015): 78.96 | Impact Factor (2015): 6.391

The Effect of Hydrogenated Amorphous Silicon on the Optical Properties of Solar Cells

Omer Abdalla Omer Gassim

College of Science and Art in Al –Mikhwah, Department of Physics, Al –Baha University, Saudi Arabia

Abstract: ***Hydrogenated amorphous silicon (a-Si:H) produced by plasma enhanced chemical vapor deposition (PECVD) is a very interesting material due to the possibility of controlling the energy band gap and the electrical properties by means of the alloy composition. In this work we focused on the intrinsic layer because it is responsible for light absorption and the subsequent charge carrier generation/separation and for photovoltaic stability under continuous illumination (Staebler–Wronski) effect. We have prepared six sample of a-Si:H (i-layer) A, B, C, D, E, F with varied H2 diluted (40, 50, 60, 70 sccm) and the deposition time is varied (30, 40 minutes) and the flow of SiH_4 was fixed at 20 sccm. The pressure of chamber MPZ (modular process zones) before deposition process about 5×10^{-7} Torr. While during deposition process is 530 mTorr, the deposition temperature is 2700C and RF power is 1.8 watt. To evaluation the optical properties of the thin film we used multiple reflection method (NanoCalc-2000 measurement system). The absorption coefficient (α) of our samples are about $1.707\times10^{-3}(nm)^{-1}$, $1.555\times10^{-3}(nm)^{-1}$, $1.312\times10^{-3}(nm)^{-1}$, $1.295\times10^{-3}(nm)^{-1}$, $1.270\times10^{-3}(nm)^{-1}$ and $1.256\times10^{-3}(nm)^{-1}$ respectively. The energy bandgap of the samples about 1.990 e.V, 1.916 e.V, 1.685 e.V, 1662 e.V, 1.594 e.V and 1.583 e.V respectively. Comparing our results with other researchers which it has the same deposition conditions but with difference deposition method (Hot Wire CVD systems) we can suggest that the efficiency of the layers (A up to F) about 6% - 9%.***

Keywords: Hydrogenated amorphous silicon (a-Si:H), plasma-enhanced chemical vapor deposition (PECVD), Staebler-Wronski effect (SWE).

1. Introduction

Recent development in thin film technology of amorphous silicon hydrogenated (a-Si:H) and its compound are becoming increasingly popular and widely used in micro structure technology and several applications such as: thin film transistor, solar cell, flat plate display, switching, multilayer's structures, ets.

Since the first observation of doping effects in hydrogenated amorphous silicon (a-Si:H) alloy, the material has received a great deal of attention as a candidate for low-cost solar cells. Amorphous semiconductors absorb sunlight very efficiently because of the inherent disorder, and only a very thin film (<500 nm) is needed to complete the solar cell structure. [1]

The average commercial crystalline silicon module increased its efficiency from about 12 to 16 percent over the last ten years but also high production costs[2][3].

The current dominance of the c-Si solar cell has its origin in the fact that c-Si is the most commonly used and investigated semiconductor material in the world. There is also great interest in thin film solar cells, since it is expected that these solar cells can be produced at lower costs, resulting in lower price-performance ratios in the near future. Furthermore, an additional advantage of thin film solar cells is that in principle they can be deposited on flexible, inexpensive substrates. Typical thin film materials used for solar cells are copper-sulphide, cadmium-sulphide, cadmium-telluride, copper indium diselinide and hydrogenated amorphous silicon. [4]

In this research work we will focus on the basis material in the hydrogenated amorphous silicon (a-Si:H) thin film for solar cell. Hydrogenated amorphous silicon is the most widely applied thin film solar cell material, due to the fact that it is widely available and the silicon material does not harm the environment.

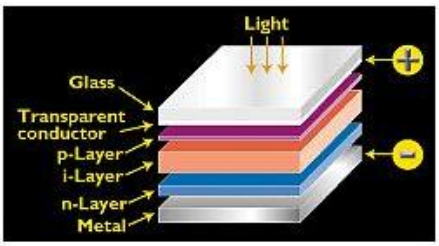

Figure 1: Schematic representation of a typical thin film a-Si:H solar cell on glass. The incoming photons with an energy larger than the band gap are absorbed in the intrinsic a-Si:H film creating holes-electron pairs .

The principle of a thin film p-i-n a-Si:H solar cell is illustrated in Figure 1. The incident light can be absorbed in the intrinsic film, which is sandwiched between p-type and n-type layers, thereby creating holes and electrons. The doped layers create an internal electric field, which serve to collect the photo-induced charge carriers. The p-layer, a-Si:H doped with boron, and the n-layer, a-Si:H doped with phosphorus, have typically a thickness of 10 nm, whereas the intrinsic a-Si:H film typically has a thickness of about 400 nm. The holes are driven towards the p-layer. The electrons are driven to the n-type layer and are collected at the metal back contact [5] [6].

The intrinsic layer is especially important because it is responsible for light absorption and the subsequent charge carrier generation/separation and for photovoltaic stability under continuous illumination (Staebler–Wronski) effect.

Concentrating on a-Si:H deposition for thin film solar cell production process the following issues are important for the price-performance ratio this are: the growth rate, the stable efficiency, large area deposition and material costs. Typically a-Si:H growth rates used in industry are about 1-3 Å/s and

based on the 13.56 MHz RFPECVD technique[7]. With these techniques it takes between ½ up to 1 hour to deposit a 400 nm thick film. Higher growth rates will lead to smaller deposition chambers and consequently lead to lower production costs. The higher the solar cells' stable efficiency the lower the price-performance ratio will be. The initial efficiency drops by 30 % under illumination due to the Staebler -Wronski effect (SWE), which is the degradation of the electro-optical a-Si:H properties under illumination. Thinner intrinsic films in a multi-junction, lower hydrogen concentration in the film and a-Si:H deposition phases close to the microcrystalline phases are possible options for improving the stability of the solar cell efficiency. Furthermore, techniques which provide higher initial efficiencies include the optimization of the single p-i-n films, interface treatments, the use of a metal back reflector and better light trapping by using textured surfaces. Next to the growth rate, the ability of a technique to deposit good film homogeneity and other film properties over large areas is very important. Aspects like the geometric limitations of a deposition technique, substrate types, demands on the pumping system, cleaning time for reactor, etc. play a key role in this issue. For the lowest material costs, processes with high gas utilization, especially for the expensive SiH_4 gas, are preferred. Furthermore, the expensive glass substrates could be replaced by cheaper thin metal foils or polymer foils.

The a-Si:H material is a random covalent network of Si-Si and Si-H bonds as show in Figure.2.

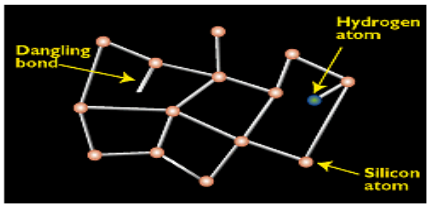

Figure 2: Amorphous silicon's random structural characteristics result in deviations like "dangling bonds" [8]

Because amorphous silicon does not have the structural uniformity of crystalline or even polycrystalline silicon, the small deviations result in defects such as dangling bonds, where atoms are missing a neighbour to which they can bond. These defects provide places for electrons to recombine with holes rather than contributing to the electrical circuit [8]. Ordinarily, such a material would be unacceptable for electronic devices because the defects limit the flow of current. But if amorphous silicon is deposited in such a way that it contains a small amount of hydrogen (through a process called "hydrogenation"), then the hydrogen atoms combine chemically with many of the dangling bonds, essentially removing them and thereby permitting electrons to move through the amorphous silicon [8][9][10].

2. Research Methodology

The substance and instrument which we used in this work is consisting from limes glass (2 mm, 10x10 cm^2), ultrasonic cleaners, Alcohol (Ethanol C_2H_5OH 70%), hydrogen dilution (H_2), plasma enhanced chemical vapor deposition system (PECVD) and nano calc-2000 measurement system for thin film. The Preparation sample is done by using limes glass with dimensions 10x10 cm^2 and thickness 2 mm.

For the process of cleaning the sample we used ultrasonic cleaners to clean the sample with alcohol (ethanol C_2H_5OH 70%) during 15 minutes. We do this step to be sure that the sample is clean from fingerprint.

Due to the deposition process all process of making single film structure (i-layer) is done on the top of the substrate limes glass.

The structure of (i-layer) single film is made by flowing SiH_4 20 sccm and H_2 is varied (40, 50, 60, 70 sccm). The pressure of chamber MPZ during process is 530 mTorr, and the deposition time is varied (30, 40 minutes), the deposition temperature is 270^0C and RF power is 1.8 watt.

The performance analysis in our work is shown to be very important in order to evaluate the optical properties of the thin film for this purpose we used multiple reflection method (NanoCalc-2000 measurement system) Figure .4. For analysis data we used MathCAD program.

We also ensure the performance data analysis in which we had analysed the data which we get from experiment to measure the absorption coefficient and the energy band gap of the i-layer using the following equations 1 and 2:

$$A = \alpha\, d \quad (1)$$

$$E_g = h\frac{c}{\lambda} \quad (2)$$

Where A is absorption; α absorption coefficient; d is the thickness of the thin film; E_g is the energy bandgap; h is Planck's constant; C is the speed of light; λ the wavelength of the light. [11]

3. Plasma Enhanced Chemical Vapour Deposition (PECVD) System

The system contains of two PECVD chambers of stainless steel construction (modular process zones or MPZ's) located around a central chamber which contains the transport system (isolation and transfer zone or ITZ), an additional load lock chamber allows introduction into the ITZ of the substrates (10x10 cm^2). The substrate carrier is moved by a transport arm which utilizes a vacuum compatible stepper motor for the linear movement, the arm rotates around a feed through placed in the center of the ITZ to position the substrate for introduction into the MPZ's. After the process the substrate is extracted from the MPZ and can be introduced into any other MPZ or taken into the load lock for unloading. The MPZ's and the load lock are separated from ITZ by means of gate valves which are open only during substrate injection and extraction from the MPZ's and the load lock. An optimization of the mechanical setup of the transport system has allowed achieve carrier transfer time between process chambers of less than two minutes. This configuration allows the deposition of layers in any sequence to produce any type of multilayer device, avoiding cross contamination between different layers [12]. A schematic diagram of the system is shown in Figure 3.

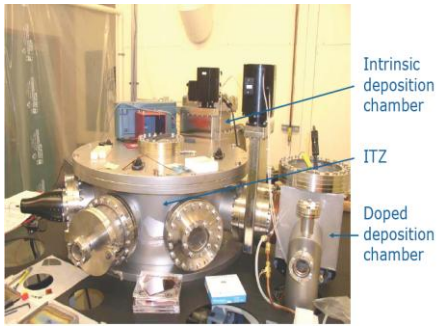

Figure 3: Schematic of the PECVD system [13]

The MPZ's are separately pumped using turbo molecular pumps and have separated gas manifolds, pumping of the process gas takes place via the turbo molecular pumps, which are equipped for use corrosive gases. Each MPZ is complete with electrodes (anode and cathode), the distance between which can be internally altered from 1 to 5 cm. The substrate is facing downwards to avoid accumulation of dust particles. Each MPZ contains rails for transportation of substrate, an ionization gauge and associated display, a heater placed outside vacuum (to avoid contamination from this source) to heat the substrate by proximity, a type K thermocouple and associated controls, a capacitance manometer gauge head, a throttle valve and relative automatic pressure controller. The MPZ's have a gas manifold containing; a radio frequency generator (13.56 MHz) and an automatic matching network are switchable between the different MPZ's to enable the PECVD process to take place.[13]

4. Experiments and Data Analysis

All process of making single film structure (i-layer) is done on the top of the substrate limes glass with dimensions 10x10 cm^2 and thickness 2 mm. We have prepared six sample of a-Si:H (i-layer) A, B, C, D, E, F with varied H_2 diluted (40, 50, 60, 70 sccm) and the deposition time is varied (30, 40 minutes) and the flow of SiH_4 was fixed at 20 sccm. The pressure of chamber MPZ during process is 530 mTorr, the deposition temperature is 270^0C and RF power is 1.8 watt. The deposition conditions of the investigated i-layers are summarized in Table.1.

Table 1: Deposition condition for i-layer of hydrogenated amorphous silicon

Layers number	Total flow rate of SiH_4 (sccm)	Total flow rate of H_2 (sccm)	Deposition time (min)	Pressure of chamber (mTorr)
A	20	40	30	530
B	20	50	30	530
C	20	50	40	530
D	20	60	30	530
E	20	70	30	530
F	20	70	40	530

After deposition the layers we used multireflection method (NanoCalc-2000 measurement system) to analyzed.

4.2 Data Analysis

Experiment is done by using system reflectormeter, so-called as Nanocalc-2000. Thickness measuring range of layer shifts out of 10 nm - 250 µ m. With help of simulation computer either determinable index of refraction and also thickness concurrently. A schematic diagram of the reflectrometer system is shown in Figure 4. Source light and reflected light is channelled with wave guide. Reference sample put at certain distance from output of wave guide causing is observed raw intensity cupola in monitor. After the intensity kept as reference data, the reference sample is changed with sample which will be measured and soon can be done gauging of spectrum reflectance. [14].

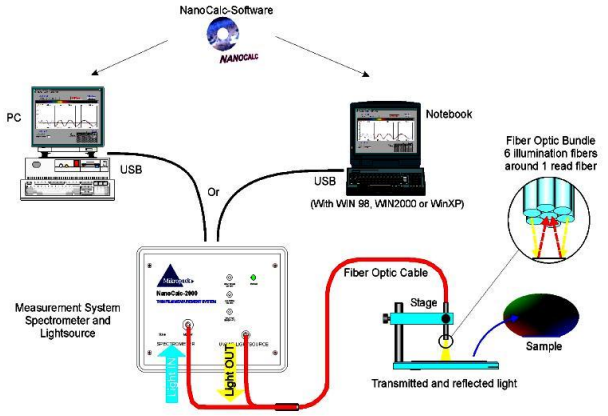

Figure 4: Schematic of the NanoCalc-2000 measurement system for thin film [14].

Data analysis can be done with software which has been provided. However, as a study process, we shall only apply result of simulation software as comparison only. We are obliged to makes simulation by using the above equations, with Microsoft Excel or other mathematics software (MathCAD program). For practicum this, layer structures is limited just for case like following:
1. Air | polymer (PMMA) | BK7glass
2. Air | polymer (MEH-PPV) | BK7glass
3. Air | SiO_2 |Si
4. Air | SiON |SiO_2

Estimate the thickness of the a-Si:H films can be obtained by Nanocalc-2000 measurement system as the fallowing:

$$R = \frac{r_1^2 + r_2^2 + 2r_1 r_2 \cos(2\delta)}{1 + r_1^2 r_2^2 + 2r_1 r_2 \cos(2\delta)} \quad (3)$$

Where R is the reflectivity; r_1 is Fresnel reflectance coefficient of the first medium (air); r_2 is Fresnel reflectance coefficient of the second medium (a-Si:H); δ is the phase difference and can be defined as:

$$\delta = \frac{2\pi}{\lambda} n_2 d \cos\theta_2 \quad (4)$$

Where n_2 is the refraction index of the second medium (a-Si:H); d the thickness of the layer; λ the wavelength of the incidence beam. For normal beam to ridge area (θ_2 = 0), so:

$$\delta = \frac{2\pi}{\lambda} n_2 d$$

And the reflectivity R will be:

$$R = \frac{r_1^2 + r_2^2 + 2r_1 r_2 \cos\left(2\frac{2\pi}{\lambda} n_2 d\right)}{1 + r_1^2 r_2^2 + 2r_1 r_2 \cos\left(2\frac{2\pi}{\lambda} n_2 d\right)} \quad (6)$$

For Fresnel reflectance coefficients r_1 and r_2 we can rewrite them for special form case of Fresnel equation with incidence angle θ_1 and θ_2 as:

$$r_1 = \frac{n_1 - n_2}{n_1 + n_2} \quad ; \quad r_2 = \frac{n_2 - n_3}{n_2 + n_3} \quad (7)$$

Where $n_1; n_2; n_3$ is the refraction index of air, (a-Si:H) and the glass respectively. The refraction index for absorbing medium consists of two parts, real and imaginary part. The real part related to speed of light in material and diffraction of light in ridge area between two medium, while the imaginary part related to absorption of light dissociation energy of diatomic by medium. Where all medium haves the character of not to permeate light (non-absorbing), namely doesn't have imaginary part in the refraction index [14].

The refraction index of (a-Si:H) as an absorbing medium is given be:

$$n_2 = n_{\text{a-Si:H}}^{\langle 1 \rangle} + i.n_{\text{a-Si:H}}^{\langle 2 \rangle} \quad (6)$$

In this work we have prepared six sample of a-Si:H (i-layer) A, B, C, D, E, F. Using Mathcad program we calculate the reflectivity R and the thickness of the layers.

4.3 The thickness, absorption coefficient and the energy bandgap: Layer A:

Table .2 The refraction index of air, a-Si:H and the glass

	0	1
0	150	1
1	151	1
2	152	1
3	153	1
4	154	1
5	155	1
6	156	1
7	157	1
8	158	1
9	159	1
10	160	1
11	161	1
12	162	1
13	163	1
14	164	1
15	165	1

n_{air}

	0	1	2
0	150	1.684	3.331
1	151	1.684	3.331
2	152	1.684	3.331
3	153	1.684	3.331
4	154	1.684	3.331
5	155	1.684	3.331
6	156	1.684	3.331
7	157	1.684	3.331
8	158	1.684	3.331
9	159	1.684	3.331
10	160	1.684	3.331
11	161	1.684	3.331
12	162	1.684	3.331
13	163	1.684	3.331
14	164	1.684	3.331
15	165	1.684	3.331

n_{aS}

	0	1
0	150	1.813
1	151	1.813
2	152	1.813
3	153	1.813
4	154	1.813
5	155	1.813
6	156	1.813
7	157	1.813
8	158	1.813
9	159	1.813
10	160	1.813
11	161	1.813
12	162	1.813
13	163	1.813
14	164	1.813
15	165	1.813

n_{BK7}

Where $n_{air} = n_1; n_{\text{a-Si}} = n_2; n_{BK7} = n_3$ and in (table 2) 0 ≡ λ the wavelength of the light, 1 ≡ $n^{\langle 1 \rangle}$ the real part of the refraction index for the medium, 2 ≡ $n^{\langle 2 \rangle}$ the imaginary part of the refraction index for the medium.

The thickness of the layer will be calculated by using Mathcad program by substitution equation 7 into equation 6 as the following:

$$R_n = \frac{\left(\frac{n_{1n}-n_{2n}}{n_{1n}+n_{2n}}\right)^2 + \left(\frac{n_{1n}-n_{3n}}{n_{1n}+n_{3n}}\right)^2 + 2\left(\frac{n_{1n}-n_{2n}}{n_{1n}+n_{2n}}\right)\left(\frac{n_{1n}-n_{3n}}{n_{1n}+n_{3n}}\right)\cos\left(2\frac{2\pi}{\lambda_n} n_{2n} d\right)}{1 + \left(\frac{n_{1n}-n_{2n}}{n_{1n}+n_{2n}}\right)^2 + \left(\frac{n_{1n}-n_{3n}}{n_{1n}+n_{3n}}\right)^2 + 2\left(\frac{n_{1n}-n_{2n}}{n_{1n}+n_{2n}}\right)\left(\frac{n_{1n}-n_{3n}}{n_{1n}+n_{3n}}\right)\cos\left(2\frac{2\pi}{\lambda_n} n_{2n} d\right)} \quad (8)$$

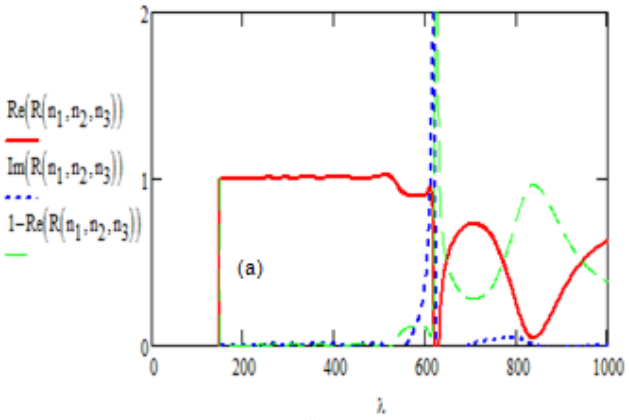

(a)

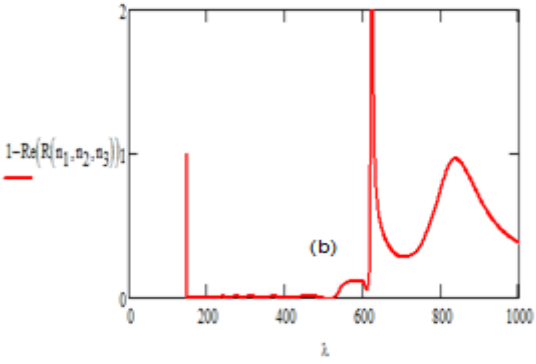

(b)

Figure 5 (a) the relationship between reflectivity R and the wavelength λ of layer A.(b) the relationship between 1-the real part of reflectivity R(absorption)and the wavelength λ of layer A.

The reflectivity R from experiment data is:

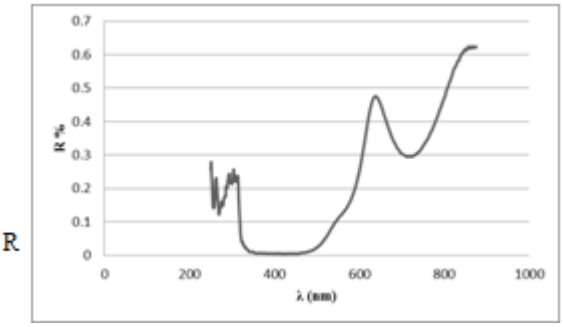

Figure 6: The relationship between1-the real part of reflectivity R and the wavelength λ of light for layer A from experiment data.

Comparing the experiment data (**figure 6**) with the calculation result by using Math CAD program (**figure 5** (a) and (b)) we found that the thickness of layer A about 300 nm. The absorption coefficient can be calculated from experiment data by using equation (1):

$$A = \alpha d$$

Where A the absorption; α absorption coefficient; d the thickness of the layer

The absorption A from experiment measurement data by using NanoCalc-2000 measurement system it found to be about 0.512 and the thickness is 300 nm, so the absorption coefficient of layer A about 1.707×10^{-3} nm (After substitute in the equation $A=\alpha d$)

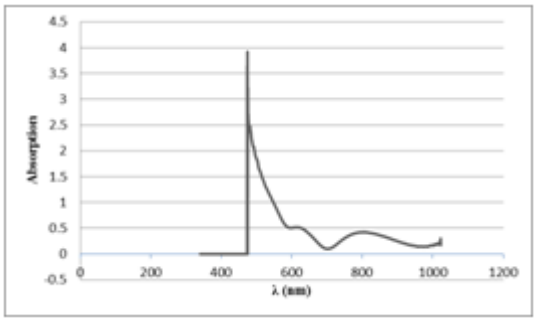

Figure 7: The relationship between absorption A and the wavelength λ of light for layer A from experiment data.

Figure 7 show the absorption (A) we get it from experiment measurement data by using NanoCalc-2000 measurement system which agreed with the calculated results by using Math CAD program. The energy bandgap can be calculated from experiment data by using equation (2):

$$E_g = h\frac{c}{\lambda}$$

E_g is the energy bandgap; h is Planck's constant; C the speed of light; λ the wavelength of the light.

$h = 6.6260693.10^{-34}\ joul.\sec$

$\lambda = 623nm$

$c = 299792458.\frac{m}{\sec}$

$e = 1.60217653.10^{-19}\ coul$

$\therefore E_g = 1.99.eV$

Table 3: The thickness, absorption coefficient, the energy bandgap and the total flow rate of H_2 for (A; B; C; D; E and F) layers

Layer number	Thickness (nm)	Absorption coefficient $(nm)^{-1}$	The energy bandgap (e.V)	Total flow rate of H_2 (sccm)
A	300	1.707×10^{-3}	1.99	40
B	310	1.555×10^{-3}	1.916	50
C	345	1.312×10^{-3}	1.685	50
D	315	1.295×10^{-3}	1.662	60
E	300	1.27×10^{-3}	1.594	70
F	350	1.256×10^{-3}	1.583	70

Table 3 summarizes the results thickness, absorption coefficient and the energy bandgap for all layers(A to F).

5. Results and Discussion

5.1 Relation between optical gap and the Hydrogen flow rate

The hydrogen concentration plays an important role in the Si:H film structure formation. In the usual type of glow discharge reactor, the resulting layers are amorphous if deposited from pure silane plasma. When we add hydrogen to the plasma, we marginally alter the layer quality, whereas the layer remains amorphous until we reach a threshold concentration. If, now, the hydrogen concentration is further increased, we start depositing crystallites, and then the crystalline volume fraction rapidly increases until we obtain layers that are essentially microcrystalline. In Figure 8 we can observe the decreasing on the energy bandgap form (1.990 e.V – 1.583 e.V) with increasing in the hydrogen flow rate from (30 sccm – 70 sccm). In the other word the increase of hydrogen concentration on the layers. The decreasing on the energy bandgap happed due to the fact that increasing of hydrogen concentration, the amorphous to microcrystalline transition takes place. If the dilution is further increased we beginning deposited crystalline [15].

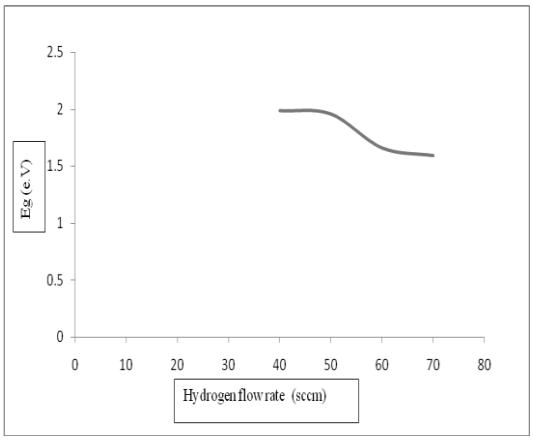

Figure 8: The relationship between Hydrogen flow rate and the energy bandgap

5.2 Relation between optical gap and the absorption coefficient

Silicon microcrystalline (µc-Si:H) is a material with an indirect bandgap (like crystalline silicon). Therefore its absorption coefficient in the visible part of the solar spectrumis relatively low, much lower than that of a-Si:H. This means that correspondingly thick µc-Si:H layers are necessary to obtain sufficient absorption and photogeneration. Figure 9 show that the absorption coefficient depends exponentially on the energy bandgap which agree with the researches which has done [16].

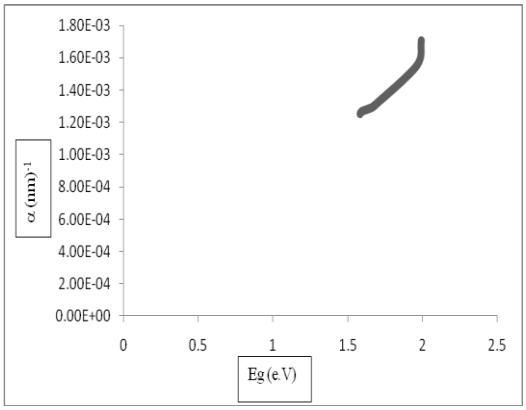

Figure 9: Relation between optical gap and the absorption coefficient

6. Conclusions

The optical properties of a-Si:H film are analysed using a multireflection method (NanoCalc-2000 measurement system) and MathCAD program. Our results show that the energy band gap depends on the microstructure and is affected differently by hydrogen bonded at vacancies or voids.

These results indeed suggest that the films deposited at 2 Å/s and high temperatures (2700C) are in between an a-Si:H and µc-Si:H structure. These deposition conditions can therefore be very attractive, because the most stable, high performance a-Si:H solar cells were obtained by a hydrogen-to-silane dilution just before the onset of microcrystallinity .

In general, the a-Si:H optical gap can be tuned by the hydrogen content. In the deposition conditions A up to F, the hydrogen content is subsequently tuned by the deposition temperature, resulting in the decreasing Eg with increasing substrate temperature. Only for low substrate temperatures (<2700C) the optical gap becomes dependent on the growth rate. The hydrogen content is related to the optical gap. The decreasing on the energy bandgap form (1.990 e.V – 1.583 e.V) with increasing in the hydrogen flow rate from (30 sccm – 70 sccm). In the other word the increase of hydrogen concentration on the layers. The decreasing on the energy bandgap happed due to the fact that increasing of hydrogen concentration, the amorphous to microcrystalline transition takes place. If the dilution is further increased we beginning deposited crystalline as shown in Fig.8, in line with reported results [17].

The absorption coefficient (α) of our samples (A up to F) are about $1.707\times10^{-3}(nm)^{-1}$, 1.555×10-3$(nm)^{-1}$, 1.312×10-3$(nm)^{-1}$, $1.295\times10^{-3}(nm)^{-1}$, $1.270\times10^{-3}(nm)^{-1}$and $1.256\times10^{-3}(nm)^{-1}$ respectively. The energy bandgap (Eg) of the samples about 1.990 e.V, 1.916 e.V, 1.685 e.V, 1662 e.V, 1.594 e.V and 1.583 e.V respectively. The thickness of the i- layer in the samples (A up to F) about 300 nm, 310 nm, 345 nm, 315 nm, 300 nm and 350 nm respectively.

Comparing our results with reported results [17] which it has the same deposition conditions but with difference deposition method (Hot Wire CVD systems) we can suggest that the efficiency of the layers (A up to F) about 6% - 9%.

References

[1] P .Rava, in: Trends in vacuum science and Technology. Research Trends, Council of Scientific Research Integration (Trivandrum, India, 1992).
[2] By Eric Wesoff, Greentech Media. "The End of Oerlikon's Amorphous Silicon Solar Saga." January 31, 2014. February 19, 2016.
[3] "Photovoltaics Report" (PDF). Fraunhofer ISE. Freiburg, 17 November 2016. Archived (PDF) from the original on 31 August 2014. Retrieved 31 August 2014.
[4] D.A. Doughty, J.R. Doyle, G.H. Lin and A. Gallagher, J. Appl. Phys. 67, 6220 (1990).
[5] "The End Arrives for ECD Solar". GreentechMedia. 14 February 2012.
[6] "Oerlikon Divests Its Solar Business and the Fate of Amorphous Silicon PV". GrrentechMedia. March 2, 2012.
[7] Kishore, R.; Hotz, C.; Naseem, H. A. & Brown, W. D. (2001), "Aluminum-Induced Crystallization of Amorphous Silicon (α-Si:H) at 150°C", Electrochemical and Solid State Letters, 4 (2): G14–G16, doi:10.1149/1.1342182.
[8] Shah, A. V.; et al. (2003), "Material and solar cell research in microcrystalline silicon", Solar Energy Materials and Solar Cells, 78 (1–4): 469–491, doi:10.1016/S0927-0248(02)00448-8.
[9] Lee, Hyun Seok; Choi, Sooseok; Kim, Sung Woo; Hong, Sang Hee (2009), "Crystallization of Amorphous Silicon Thin Film by Using a Thermal Plasma Jet", Thin Solid Films, 517 (14): 4070–4073, Bibcode:2009TSF...517.4070L, doi:10.1016/j.tsf.2009.01.138.
[10] "An analysis of the energy efficiency of photovoltaic cells in reducing CO2 emmisions". University of Portsmouth. 31 May 2009. Archived from the original on 25 March 2015. Energy Pay Back time comparison for Photovoltaic Cells (Alsema, Frankl, Kato, 1998, p. 5.
[11] A. Madan, P. Rava, R.E.I. Schropp and B.Von Rocdern, MV systems Inc, 327 Lamb Lane, Golden, CO 80401. USA (1992).
[12] Onno Gabriel, Simon Kirner , Michael Klick, Bernd Stannowski, Rutger Schlatmann, "Plasma monitoring and PECVD process control in thin film silicon-based solar cell manufacturing." EPJ Photovoltaics 5, 55202 (2014), www.epj-pv.org DOI: 10.1051/epjpv/2013028.
[13] K. Takahashi and M. Konagi, Amorphous silicon solar cells, Tokyo Institute of Technology (1986)
[14] Karakterisasi Sifat Optik Lapisan Tipis Lewat Metoda Pemantulan Jamak, KK Fisika Magnetik Dan Fotonik, FMIPA – Institute Technology Bandung (ITB).
[15] H.M. Branz, Phys. Rev. B 59, 5498 (1999).
[16] F. finger, U. Kroll, V. Viret, A. Shah, W. Beyer, X.-M. Tang, J. Weber, A. Howling, and Ch. Hollenstein, J. Appl. Phys. 71, 5665 (1992).
[17] P. Kea-Nune, J. Perrin, J. Guillon, and J. Jolly, Plasma Sources Sci.Technol. 4, 250 (1995).